Nuclear structure of ^{18}N and the neighboring $N = 11$ isotones

M. Wiedeking,[1] P. Fallon,[1] A. O. Macchiavelli,[1] L. A. Bernstein,[2] J. Gibelin,[1] L. Phair,[1] J. T. Harke,[2] D. L. Bleuel,[2] R. M. Clark,[1] M-A. Deleplanque,[1] S. Gros,[1] R. Hatarik,[3] H. B. Jeppesen,[1] I-Y. Lee,[1] B. F. Lyles,[2,4] M. A. McMahan,[1] L. G. Moretto,[1,5] J. Pavan,[1] E. Rodriguez-Vieitez,[1,4] and A. Volya[6]

[1]*Lawrence Berkeley National Laboratory, Berkeley, California 94720, USA*

[2]*Lawrence Livermore National Laboratory, Livermore, California 94550, USA*

[3]*Rutgers University, Department of Physics and Astronomy, Piscataway, New Jersey 08854, USA*

[4]*Department of Nuclear Engineering, University of California, Berkeley, California 94720, USA*

[5]*Department of Chemistry, University of California, Berkeley, California 94720, USA*

[6]*Florida State University, Department of Physics, Tallahassee, Florida 32306, USA*

(Received 29 June 2007; revised manuscript received 12 December 2007; published 5 May 2008)

The fusion-evaporation reaction ^{9}Be(^{11}B,2p) was used to populate excited states in ^{18}N. New gamma-ray transitions were added to the ^{18}N level scheme. The mean lifetime of the first excited state was measured to be 582(165) ps and its transition rate to the ground state was determined to be $B(M1) = 0.036(10)$ W.u. Shell model calculations in the full *p-sd* model space were used to investigate the low-lying configurations in ^{18}N and in the $N = 11$ isotones ^{17}C and ^{19}O. It was found that the role of the proton-neutron interaction is important in determining the ground state and low-lying excited state properties. The ground state spin inversion in these isotones is attributed to the increased importance of the quadrupole relative to the pairing interaction and is discussed within the framework of a schematic pairing + quadrupole model.

DOI: 10.1103/PhysRevC.77.054305 PACS number(s): 21.10.Tg, 21.60.Cs, 23.20.−g, 27.20.+n

I. INTRODUCTION

Neutron-rich *p-sd* shell nuclei display a variety of phenomena that include: a reduction in the *p-sd* shell gap for neutron-rich O and F isotopes [1], the onset of large deformations in ^{17}C ($\beta_2 = 0.52(4)$) [2] and ^{17}B ($\beta_2 = 0.57(5)$) [3], and a neutron halo structure in ^{14}B [4]. ^{18}N has one proton hole and three neutrons outside the $N = Z = 8$ core and is also sufficiently far from stability to amplify the effects of neutron excess on the nuclear structure, yet it is still within the reach of fusion reactions at stable beam facilities. One effect of current interest is the role of the proton-neutron interaction and its influence on nuclear shell structure (see Refs. [5,6] for recent discussions). Indeed, it has been known for a long time [7] that the interaction between valence neutrons and protons plays a pervasive role in the evolution of nuclear structure with changing neutron and proton number as discussed by Refs. [8–10]. The *monopole* component of the proton-neutron interaction can cause large shifts in the single-particle energies (SPE) that may significantly change the underlying spherical shell structure, while the *quadrupole* component provides a mechanism to develop deformation and collectivity away from closed shells. Changes in the single-particle energies due to the monopole interaction can in turn modify the available valence space and influence the onset and strength of collective modes.

In this paper we report data on gamma-ray decays of ^{18}N excited states and a measurement of the lifetime of the first excited state in ^{18}N populated in a fusion-evaporation reaction using a plunger technique. We discuss the structure of ^{18}N and the role of valence proton-neutron interactions in describing its ground-state and excited-state properties as well as those of the neighboring $N = 11$ isotones ^{19}O and ^{17}C. The ground state spin inversion in these isotones is attributed to the increased importance of the quadrupole relative to the pairing interaction and discussed within the framework of a schematic pairing + quadrupole model.

Previous experiments to study ^{18}N used beta-decay [11–14] and charge-exchange reactions [15,16]. Reference [11] also carefully examines shell model results and observed levels in ^{18}N. The only information on excited state transition rates came from the beta-decay study [12] that suggested, based on intensity balance arguments, a long mean lifetime for the ^{18}N first excited state of greater than 600 ns, in disagreement with both shell model predictions and neighboring systematic trends. The use of a fusion-evaporation reaction enables a direct measurement of the lifetimes of low-lying levels from observed Doppler shifted gamma-ray energies.

II. EXPERIMENTS

The experiment was carried out in two separate measurements at the 88-Inch Cyclotron at Lawrence Berkeley National Laboratory using the ^{9}Be(^{11}B,2p)^{18}N fusion-evaporation reaction at a beam energy of 50 MeV. The first measurement provided data on the gamma decay of excited states, the second was used to extract the lifetime of the 2^- first excited state. In both measurements the emitted γ-radiation and charged-particles were detected with the STARS-LIBERACE detector array, which consists of large area segmented annular silicon detectors (in a ΔE-E telescope arrangement) and up to six HPGe Clover detectors [17,18]. The large proton binding energy exhausted the available excitation energy and suppressed the evaporation of additional neutrons in conjunction with the 2p channel at the chosen beam energy. The 2p coincidence cleanly selected the weak (∼0.2 mb) ^{18}N channel from the total ∼800 mb cross section estimated for fusion channels

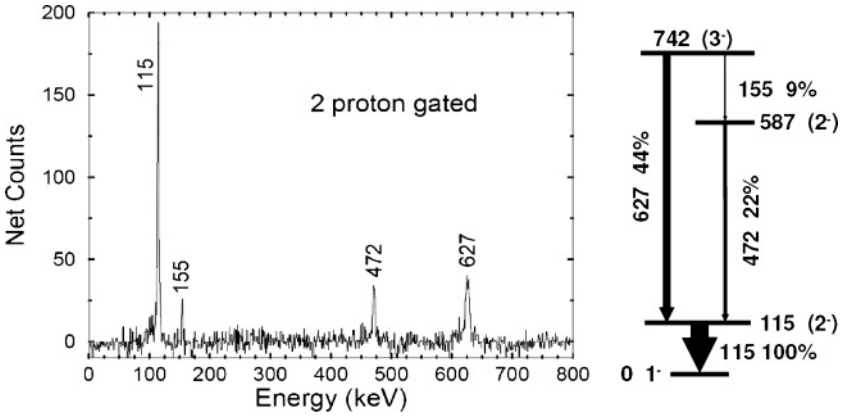

FIG. 1. (Left) Two proton gated γ-ray spectrum, after subtraction of random γ-particle events. The transitions at 115, 155, 472, and 627 keV are decays from ^{18}N excited states. The dispersion is 1 keV/channel and the uncertainty in γ-ray energy is 1 keV. (Right) Levels in ^{18}N observed from this work. The transitions at 627 and 155 keV are observed for the first time. Transition intensities are given next to the energy, normalized to the 115 keV transition. Line widths are proportional to the intensities. Spin assignments are from previous works [11,16].

(cross sections are taken from PACE [19] statistical model estimates). The gamma-ray photopeak detection efficiency was 1% at 1 MeV. The efficiency for detecting one-proton in the silicon array was 20%. Germanium detector energy and efficiency calibrations were performed using a ^{152}Eu γ-ray source. Silicon detectors were calibrated with an α emitting ^{226}Ra source.

III. EXPERIMENT 1 SETUP

The measurement of the spectrum and decay of ^{18}N excited states used five Clover germanium detectors placed 16.5 cm from the target. Two detectors were located at 90°, two at 140°, and one at 40° relative to the beam direction. The charged-particle telescope consisted of a 152 μm ΔE detector and 1000 μm E detector separated by 3 mm. The silicon detector telescope was mounted 3.0 cm downstream from the target. A 56.7 mg/cm^2 thick ^{nat}Pb foil (97% purity) spanned the front of the ΔE detector to suppress α-particles from ^{9}Be breakup. The ^{9}Be (99.0% purity) target thickness was 2.6(1) mg/cm^2, as determined from energy loss measurements of ^{210}Po α particles through the target. The average beam current was 0.5 pnA over a period of 5 d. The online trigger required detection of at least two charged-particles within a coincidence interval of ∼400 ns. Gamma-ray events were recorded to disk if they were associated with a valid particle trigger. In the offline analysis the particle-particle coincidence interval was reduced to ∼100 ns, and a time gate between the γ-ray and two-particle trigger was used to reject uncorrelated γ-particle-particle events.

IV. EXPERIMENT 2 SETUP

The lifetime of the first excited state was measured using the recoil distance method [20]. A 1.35(5) mg/cm^2 ^{9}Be (99.8% purity) self-supporting target was separated from a 56.7 mg/cm^2 ^{nat}Pb stopper foil (99.99% purity) by a set of fixed distance spacers. A range of spacer thicknesses from 0.08 to 3 mm was available. For this measurement we used the 1.0(1) and 3.0(1) mm spacers. Five Clover germanium detectors were placed 16.5 cm from the target: two detectors were located at 40°, two at 140°, and one at 90° relative to the beam direction. The charged-particle telescope setup was similar to that used in experiment 1. The online trigger required detection of at least one charged-particle within a coincidence interval of ∼200 ns. A 100 ns time gate between the γ-ray and master trigger and between the two protons themselves was used to reject uncorrelated γ-p-p events in the offline analysis. Data were taken for approximately 12 h at the 1 mm target-stopper distance and for 2 d at the 3 mm distance. The average beam current was 0.3 pnA. In both measurements the beam current was limited by the silicon detector rate.

V. RESULTS

The two-proton gated, Doppler corrected, γ-ray spectrum of ^{18}N is shown in Fig. 1. The four lines at 115, 155, 472, and 627 keV are assigned to decays of ^{18}N excited states, as shown in the level scheme. The transitions at 155 and 627 keV are observed for the first time. $2p$ gated γ-γ coincidence spectra are shown in Fig. 2. The measured coincidences together with the relative γ-ray intensities help to unambiguously assign the γ-decays to states in ^{18}N.

Figure 3 shows non-Doppler corrected gamma-ray spectra for ^{18}N ($2p$ channel) and ^{16}N ($1p1t$ channel) for detectors at 140° and 40° obtained at a target-stopper distance of

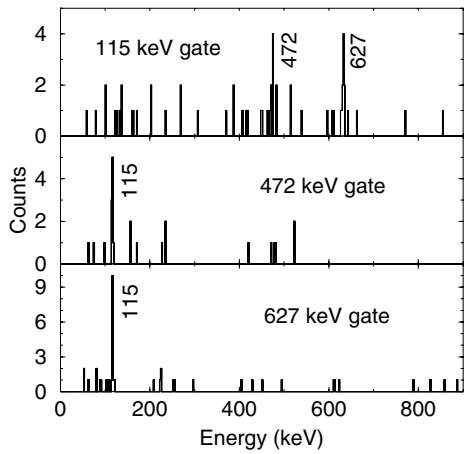

FIG. 2. Two-proton-γ-γ coincidence spectra obtained by gating on transitions at 115 (top panel), 472 (middle panel), and 627 keV (lower panel). The 472 and 627 keV transitions are shown to be in coincidence with the 115 keV line. The dispersion is 2 keV/channel.

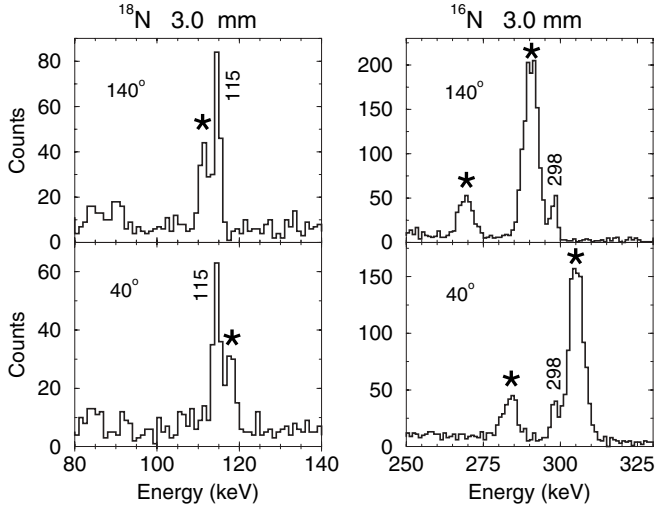

FIG. 3. Gamma-ray spectra for detector angles at 140° and 40° obtained at the 3.0(1) mm target-stopper distance for ^{18}N (left two columns) and ^{16}N. (right two columns). Two-proton (^{18}N) gated spectra and one-proton, one-triton (^{16}N) gated spectra are shown. Stars indicate moving peak components. The dispersion is 1 keV/channel.

3.0(1) mm. ^{16}N has a 3^- state decaying via a 298 keV γ-ray with a mean lifetime of 131.7(19) ps [21], and a 1^- state decaying via a 277 keV γ-ray with a mean lifetime of 5.63(5) ps [21]. The ^{16}N 298 keV γ-ray provides an internal calibration for lifetimes extracted in this experiment. At a target-stopper foil distance of 3 mm both the ^{18}N 115 keV and ^{16}N 298 keV γ-rays have moving and stopped components, while the 277 keV ^{16}N peak has only a moving component. Doppler shifted components are marked by a star. The average velocities of the ^{18}N and ^{16}N recoiling nuclei were measured to be $v/c = 0.037(6)$ and $v/c = 0.031(3)$, respectively, from observed Doppler shifted γ-ray energies. State lifetimes were determined using the relation $N/N_0 = e^{-(t/\tau)}$; where N is the number of counts in the stopped γ-ray peak, N_0 is the sum of the moving and stopped peaks, t is the average time taken for the recoil to traverse the gap between the target and stopper foils, and τ is the mean lifetime. The ratio $N/N_0 = 62(11)\%$ for the ^{18}N 115 keV gamma-ray yields a mean lifetime of 582(165) ps for the ^{18}N first excited 2^- state. The ^{16}N 298 keV transition has a ratio $N/N_0 = 11(1)\%$ (Fig. 3) giving a lifetime of 145(16) ps for the 3^- state in good agreement with the reported value of 131.7(19) ps [21], while the 277 keV transition in ^{16}N is observed to be fully shifted as expected for a mean lifetime of 5.63(5) ps [21].

The lifetime values reported here assume a single exponential decay curve, which is valid for feeding (life) times far shorter than the state lifetime. The agreement with the ^{16}N adopted values supports this assumption. In this measurement observed feeding accounts for 66(5)% of the total intensity of the ^{18}N 115 keV transition with the remaining intensity coming from unobserved side feeding. The two transitions feeding the first excited 2^-level (Fig. 1) are fully shifted at the 3.0 and also at the 1.0 mm distance implying their mean lifetimes are shorter than ~40 ps (<10% level). A 40 ps feeding lifetime (upper limit) would reduced the ^{18}N 2^- lifetime by only a few ps much less than the quoted uncertainties.

Data taken at the 1.0 mm target-stopper distance show a small (<15%) moving component, consistent with $\tau =$ 582(165) ps obtained above; however, due to the reduced statistics and larger uncertainties at the 1 mm compared to the 3 mm distance these data are not included in our final analysis.

The measured lifetime for the 115 keV state corresponds to a $B(M1)$ transition rate of 0.036(10) W.u. It rules out any significant $E2$ component as this would imply an unreasonably large $B(E2)$ value (several thousand W.u.).

VI. DISCUSSION

We begin this section by discussing the $N = 11$ isotones ^{17}C, ^{18}N, and ^{19}O within the framework of the seniority model and a simple but pedagogically instructive pairing plus quadrupole model. This is followed by more appropriate shell model calculations and a discussion of the underlying structure of the levels in ^{18}N by analyzing the results of the $B(M1)$ measurement. We end this section with a brief discussion on the connection between the pairing plus quadrupole and shell model.

The measured ^{18}N excitation spectrum is compared with the neighboring $N = 11$ isotones ^{19}O and ^{17}C in Fig. 4. With three valence neutrons outside the $N = 8$ core the simplest neutron configuration for these nuclei would involve $\upsilon(d_{5/2})^3$ coupled to either $J = 5/2$ or $J = 3/2$. ^{18}N has a

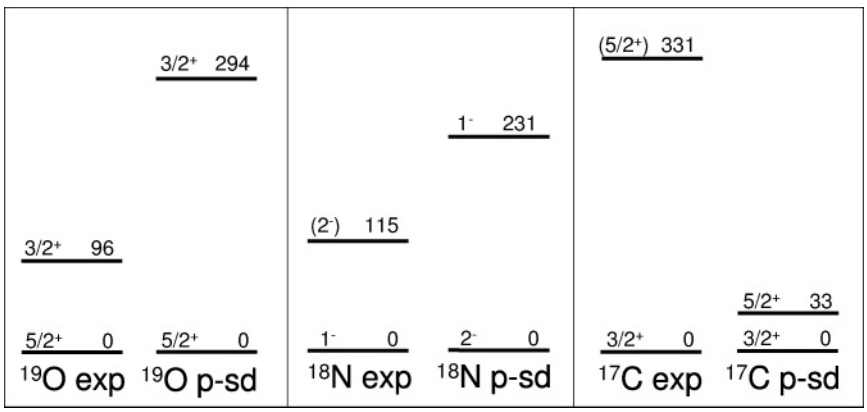

FIG. 4. ^{19}O [22], ^{18}N, and ^{17}C [2] low-lying experimental (labeled exp) and corresponding shell model results (labeled p-sd) utilizing the "full p-sd" model space (see text for details). The 210 keV level [2] (tentative $1/2^+$ state) in ^{17}C is not shown.

1^- ground state (Fig. 1), which requires the $(d_{5/2})^3$ neutrons to couple to $J = 3/2$. Alternatively, one valence neutron in ^{18}N could occupy the $s_{1/2}$ state $[\upsilon(d_{5/2})^2(s_{1/2})^1]$ leading to a neutron $J = 1/2$ configuration. Coupling this neutron $J = 1/2$ configuration to the odd $p_{1/2}$ proton then gives a 1^-state. However, a pure neutron configuration involving the $s_{1/2}$ orbit is not supported by experiment since it leads to an $L = 2\,M1$ forbidden transition from the $2^- \rightarrow 1^-$ state.

In ^{19}O the paired neutron $\upsilon(d_{5/2})^3$ configuration for the $5/2^+$ [22] ground state is favored while in ^{17}C the unpaired $\upsilon(d_{5/2})^3$ configuration is favored for the $3/2^+$ ground state [2,17]. ^{18}N has a 1^- ground state which requires neutrons coupled to $J = 3/2$ suggesting unpaired $(d_{5/2})^3$ neutrons. The $N = 11$ isotones ^{19}O, ^{18}N, and ^{17}C in Fig. 4 thus exhibit a change from a paired to unpaired neutron coupling scheme, with ^{18}N being the transitional nucleus.

At this point it is instructive to consider a simple pairing plus quadrupole (P+Q) model for the three neutrons within the $d_{5/2}$ orbit [23]. In this model the energy is given by $E = -V_0\delta_{(1,0)} + xP_2$; V_0 is the strength of the pairing interaction $\delta_{(1,0)}$ and x is the strength of the quadrupole interaction P_2. Figure 5 shows the energy of the $\upsilon(d_{5/2})^3$ $3/2^+, 5/2^+$, and $9/2^+$ states as a function of the ratio x/V_o. An increasing ratio x/V_o corresponds to the increasing importance of the quadrupole interaction, which in turn can be interpreted as an increase in deformation. For a pairing dominated system $(x/V_o = 0)$ the paired $5/2^+$ state is favored and the $3/2^+$, and $9/2^+$ unpaired states are degenerate. As the strength of the quadrupole interaction is increased relative to the pairing interaction, the $3/2^+$ and $9/2^+$ states split and the $3/2^+$ state approaches the $5/2^+$ until at $x/V_o = 1$ they become degenerate. For $x/V_o > 1$ the $3/2^+$ state is favored. Comparing Figs. 4 and 5, we find that ^{19}O would then correspond to the case $x/V_o < 1$ (paired, lower deformation), ^{18}N with $x/V_o \sim 1$, and ^{17}C with $x/V_o > 1$ (unpaired, larger deformation). The switch in ground state spin between ^{19}O and ^{17}C is then interpreted as a consequence of an increasing quadrupole strength relative to pairing, which implies an increase in deformation. This is consistent with the measured deformations, $\beta_2 = 0.006(1)$ and $\beta_2 = 0.52(4)$ for ^{19}O [24] and ^{17}C [2], respectively.

From the seniority model the unique 1^- and 3^- states in ^{18}N (Fig. 1) correspond to an unpaired (seniority $s = 3$) and a paired ($s = 1$) neutron configuration, respectively. One of the two 2^- states corresponds to the $s = 3$ and the other one to the $s = 1$ configuration. Seniority (number of unpaired nucleons) is an exact quantum number [9,25] in the $\upsilon(d_{5/2})^3$ valence space (with $j \leqslant 7/2$) regardless of the interaction. From the seniority selection rules [9] $M1$ transitions ($\Delta s = 0$) are allowed for $3^-(s = 1) \rightarrow 2^-(s = 1)$ and $2^-(s = 3) \rightarrow 1^-(s = 3)$. Similarly, $E2$ transitions ($\Delta s = 1$) are allowed for $3^-(s = 1) \rightarrow 2^-(s = 3)$, $3^-(s = 1) \rightarrow 1^-(s = 3)$, and $2^-(s = 1) \rightarrow 2^-(s = 3)$. As shown later, we can use the $B(M1)$ value obtained in this measurement to assign seniority numbers to the observed 2^- states. Shell model calculations were carried out in the full p-sd model space using the code COSMO [26,27]. The calculations utilize the WBP [28] interaction with p-shell, p-sd cross shell, and sd-shell interactions in both the $T = 0$ (np) and $T = 1(nn, pp)$ channels, allowing the nucleons to move freely in or out of any p-sd orbit. A detailed shell model analysis on nuclear levels in ^{18}N using different interactions can be found in Ref. [11]. The p-sd shell model reproduces the transition from a paired to unpaired $\upsilon(d_{5/2})^3$ ground state when going from ^{19}O to ^{17}C (Fig. 4), although it tends to overestimate the relative binding of the paired neutron configuration by 200–300 keV; i.e., the $3/2^+$ state is too high in ^{19}O, the $5/2^+$ state is too low in ^{17}C, and the 1^- and 2^- states in ^{18}N are inverted, relative to experimental data. The measured ^{18}N levels are shown in Fig. 6 (left) together with shell model calculation (right). The calculation shows overall agreement with the low-energy level structure and the spin-parity assignments [11,12,16] for the four lowest states. The reversal in the ground-state and excite-state spins, compared with experiment, is discussed above. Calculated configurations and $B(M1)$ values for the lowest four states are

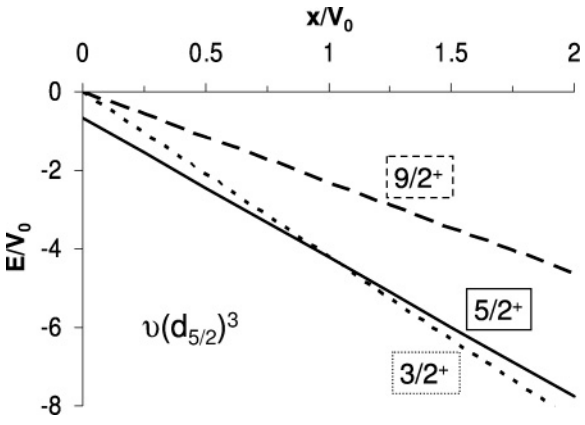

FIG. 5. Effect of varying the relative strengths of pairing $(V_o\delta_{(1,0)})$ and quadrupole (xP_2) forces for three neutrons in the $d_{5/2}$ level. The $3/2^+$ and $5/2^+$ states cross at $x/V_o = 1$. To the left side of the crossing the pairing force dominates and to the right the quadrupole force dominates.

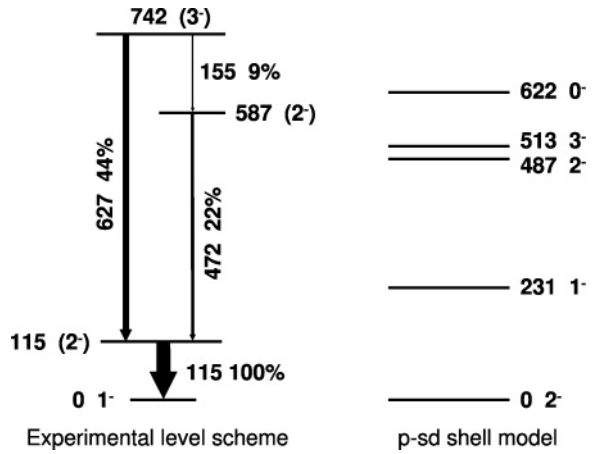

FIG. 6. (Left) Low-energy levels in ^{18}N as observed in this work. (Right) Low-lying negative-parity states predicted by the shell model code COSMO [26,27] utilizing the full p-sd model space. The next higher lying state above the 622 keV level is predicted at 1167 keV.

TABLE I. Shell model (*p-sd*) configurations and $B(M1)$ values for the four lowest states in ^{18}N. I^π is the spin and parity of the states and the *p-sd* configurations show the occupation probabilities. $I_i^\pi \rightarrow I_f^\pi$ indicates the transition from an initial to a final state of spin I and parity π. $B(M1)_{\text{th}}$ is the calculated magnetic dipole transition strength.

I^π	*p-sd* configurations	$I_i^\pi \rightarrow I_f^\pi$	$B(M1)_{\text{th}}$ W.u.
1^-	$47\% : \pi(p_{1/2})^1 \otimes \upsilon(d_{5/2})^3$		
	$36\% : \pi(p_{1/2})^1 \otimes \upsilon(d_{5/2})^2(s_{1/2})^1$		
2_1^-	$68\% : \pi(p_{1/2})^1 \otimes \upsilon(d_{5/2})^3$	$2_1^- \rightarrow 1^-$	0.0545
	$16\% : \pi(p_{1/2})^1 \otimes \upsilon(d_{5/2})^1(s_{1/2})^2$		
2_2^-	$48\% : \pi(p_{1/2})^1 \otimes \upsilon(d_{5/2})^3$	$2_2^- \rightarrow 1^-$	0.0033
	$34\% : \pi(p_{1/2})^1 \otimes \upsilon(d_{5/2})^2(s_{1/2})^1$	$2_2^- \rightarrow 2_1^-$	0.1849
3^-	$69\% : \pi(p_{1/2})^1 \otimes \upsilon(d_{5/2})^3$	$3^- \rightarrow 2_1^-$	0.0006
	$17\%: \pi(p_{1/2})^1 \otimes \upsilon(d_{5/2})^1(s_{1/2})^2$	$3^- \rightarrow 2_2^-$	0.1256

given in Table I. In the *p-sd* shell model the 1^- configuration is calculated to be highly mixed with neutrons occupying both the $d_{5/2}$ and $s_{1/2}$ orbits (Table I). A spin 2^- state can arise from both the $J = 5/2$ or $J = 3/2$ $\upsilon(d_{5/2})^3$ configurations leading to a state with either paired or unpaired neutron contribution, respectively. The shell model calculation predicts the lowest 2_1^- state to be mainly $\upsilon(d_{5/2})^3$, while the next 2_2^- state is an approximate equal mixture of $\upsilon(d_{5/2})^3$ and $\upsilon(d_{5/2})^2(s_{1/2})^1$.

The $B(M1)$ value for the ^{18}N 115 keV state is shown in Fig. 7 together with results from "full" and "restricted" *p-sd* shell model calculations. Also shown for reference is the $B(M1)$ value for ^{19}O [22]. The full calculation allows all possible two-body interactions within the *p-sd* valence space (i.e., *nn*, *pp*, *np*), while the restricted model space calculation treats the protons as a closed core and only valence neutron interactions (*nn*) are allowed. Freezing the proton configuration and allowing only valence neutrons to be active results in a reduced $2_1^- \rightarrow 1^-$ transition rate, compared with experiment (a similar effect occurs if only protons are active). Allowing the full range of interactions, specifically the proton-neutron interaction, increases the calculated $B(M1)$ value and provides better agreement with the measured value (although

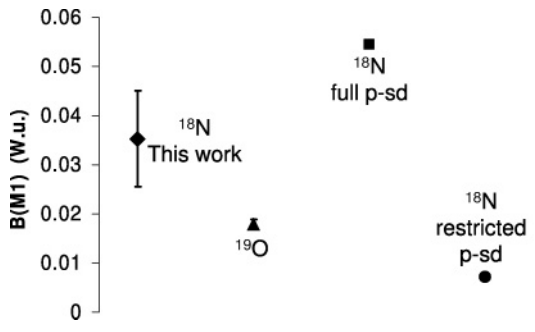

FIG. 7. Comparison of $B(M1)$ values for the 115 keV excited state in ^{18}N obtained from (i) this experiment (diamond), (ii) full *p-sd* model space calculations (square), and (iii) restricted *p-sd* model space calculations (circle), where no proton holes are allowed in the $p_{3/2}$ orbit. Also included is the value for ^{19}O [22] (triangle).

it now overestimates the data somewhat). This underlines the importance of the proton-neutron valence interaction. We note, the full shell model calculation gives a ground state magnetic moment $\mu = 0.2890\,\mu_N$ in comparison to the measured values, $|\mu| = 0.3279(13)\,\mu_N$ [13] and $|\mu| = 0.135(15)\,\mu_N$ [14].

The $B(M1 : 2^- \rightarrow 1^-)$ value can be used to assign a configuration to the first excited 2^- state. As a result of seniority selection rules $M1$ transitions are forbidden between states of different seniority [9] and this can be used to distinguish between the two possible configurations. This selection rule is violated by seniority mixing as evidenced by the observed $M1$ decay of the first excited state ($s = 3$) to ground state ($s = 1$) in ^{19}O [22]. Therefore the ^{19}O result sets a scale ($\sim$0.02 W.u.) for the amount of "forbidden" $B(M1)$ due to seniority mixing. Our measurement of $B(M1) = 0.036(10)$ W.u. displays a hindrance of the same order as that reported in ^{19}O, thus supporting the neutron $s = 1$, $J = 5/2$ assignment to the first 2^- state in ^{18}N. We recall that the $M1$ transition from the 2_1^- state to the 1^- ground state is not sensitive to components involving the $s_{1/2}$ orbit since it leads to an $L = 2$ $M1$ forbidden transition from the $2^- \rightarrow 1^-$ state.

We end this section with a discussion on the connection between shell model and the P+Q model results. Within the framework of the P+Q model the ground-state spin inversion can be attributed to an increasing deformation. The shell model tells us that proton-neutron valence interactions play a key role in determining the ground and excited state properties of ^{18}N and ^{17}C. In particular a small percentage of $p_{3/2}$ proton holes interacting with the $d_{5/2}$ neutrons appear to be mainly responsible for the observed transition strengths and level structure in these nuclei. This percentage, albeit small, increases for ^{17}C as a proton is removed from ^{18}N and suggests the increase in quadrupole force originates from the motion of protons in the *p*-shell and the resulting proton-neutron interaction. This is consistent with theoretical predictions that deformation in these light nuclei is practically impossible with one type of nucleon due to the limited kinematics of the small space involved [25]. It is known [5,29] that the $\Delta l = 1$ (tensor) proton-neutron interaction is attractive between states with $j_> = l_1 + 1/2$ and $j_< = l_2 - 1/2$ (it is repulsive for other cases). It is interesting to speculate that removing protons from the $p_{1/2}(j_<)$ state, which act on the $d_{5/2}(j_>)$ neutrons, would modify the neutron *sd* shell level spacing sufficiently to cause the onset of large quadrupole deformations and the switch in ground state spins in ^{18}N and ^{17}C. Further experimental and theoretical investigations are of interest to understand the connection between the monopole and quadrupole proton-neutron interactions and the evolution of deformation in this region away from stability.

VII. SUMMARY

^{18}N has been studied in the fusion-evaporation reaction ^{9}Be(^{11}B,2*p*) at 50 MeV using the STARS-LIBERACE detector array at the LBNL 88-Inch Cyclotron. The measurement demonstrates the feasibility to cleanly extract and study light neutron-rich nuclei, produced with low cross-sections, using the two-proton fusion-evaporation channel. Two new γ-transitions decaying from the 742 keV excited state were

observed and their placement is supported by γ-γ coincidence measurements. The lifetime of the first excited state in ^{18}N was measured to be 582(165) ps using the recoil distance method, which corresponds to a $B(M1) = 0.036(10)$ W.u. This "hindered" $M1$ transition rate is similar to the value reported in ^{19}O and suggests a seniority forbidden transition from the $2_1^-(s = 1) \rightarrow 1^-(s = 3$ g.s.) in ^{18}N. The ground-state spin inversion from a paired to unpaired neutron $(d_{5/2})^3$ coupling scheme observed in the $N = 11$ isotones ^{17}C, ^{18}N, and ^{19}O is attributed to the increased importance of the quadrupole relative to the pairing interaction. Shell model calculations carried out in the full *p-sd* space show good agreement with the data and indicate that the proton-neutron interaction plays a key role in determining the excited and ground state properties in these nuclei. It will be of interest to further pursue the interplay between valence proton-neutron interactions and the evolution of deformation in these light neutron-rich nuclei.

ACKNOWLEDGMENTS

The authors thank the operations staff of the 88-Inch Cyclotron. For Lawrence Berkeley National Laboratory this work was supported by the Director, Office of Science, Office of Nuclear Physics, of the US Department of Energy under Contract no. DE-AC02-05CH11231. Part of this work was performed under the auspices of the US Department of Energy by the University of California, Lawrence Livermore National Laboratory under Contract no. W-7405-Eng-48 and under Contract no. DE-AC52-07NA27344.

[1] M. Wiedeking, S. L. Tabor, J. Pavan, A. Volya, A. L. Aguilar, I. J. Calderin, D. B. Campbell, W. T. Cluff, E. Diffenderfer, J. Fridmann, C. R. Hoffman, K. W. Kemper, S. Lee, M. A. Riley, B. T. Roeder, C. Teal, V. Tripathi, and I. Wiedenhöver, Phys. Rev. Lett. **94**, 132501 (2005).

[2] Z. Elekes, Zs. Dombrádi, R. Kanungo, H. Baba, Zs. Fülöp, J. Gibelin, Á. Horváth, E. Ideguchi, Y. Ichikawa, N. Iwasa, H. Iwasaki, S. Kanno, S. Kawai, Y. Kondo, T. Motobayashi, M. Notani, T. Ohnishi, A. Ozawa, H. Sakurai, S. Shimoura, E. Takeshita, S. Takeuchi, I. Tanihata, Y. Togano, C. Wu, Y. Yamaguchi, Y. Yanagisawa, A. Yoshida, and K. Yoshida, Phys. Lett. **B614**, 174 (2005).

[3] Zs. Dombradi, Z. Elekes, R. Kanungo, H. Baba, Zs. Fülöp, J. Gibelin, Á. Horváth, E. Ideguchi, Y. Ichikawa, N. Iwasa, H. Iwasaki, S. Kanno, S. Kawai, Y. Kondo, T. Motobayashi, M. Notani, T Ohnishi, A. Ozawa, H. Sakurai, S. Shimoura, E. Takeshita, S. Takeuchi, I. Tanihata, Y. Togano, C. Wu, Y. Yamaguchi, Y. Yanagisawa, A. Yoshida, and K. Yoshida, Phys. Lett. **B621**, 81 (2005).

[4] E. Sauvan, F. Carstoiu, N. A. Orr, J. C. Angélique, W. N. Catford, N. M. Clarke, M. Mac Cormick, N. Curtis, M. Freer, S. Grévy, C. Le Brun, M. Lewitowicz, E. Liégard, F. M. Marqués, P. Roussel-Chomaz, M. G. Saint Laurent, M. Shawcross, and J. S. Winfield, Phys. Lett. **B491**, 1 (2000).

[5] T. Otsuka, T. Matsuo, and D. Abe, Phys. Rev. Lett. **97**, 162501 (2006).

[6] R. B. Cakirli and R. F. Casten, Phys. Rev. Lett. **96**, 132501 (2006).

[7] A. de Shalit and M. Goldhaber, Phys. Rev. **92**, 1211 (1953).

[8] I. Talmi and I. Unna, Annu. Rev. Nucl. Sci. **10**, 353 (1960).

[9] A. de Shalit and I. Talmi, *Nuclear Shell Theory* (Academic Press, New York, 1963).

[10] R. F. Casten, *Nuclear Structure from a Simple Perspective* (Oxford University Press, Oxford, 1990).

[11] J. W. Olness, E. K. Warburton, D. E. Alburger, C. J. Lister, and D. J. Millener, Nucl. Phys. **A373**, 13 (1982).

[12] M. S. Pravikoff, F. Hubert, R. Del Moral, J.-P. Dufour, A. Fleury, D. Jean, A. C. Mueller, K.-H. Schmidt, K. Sümmerer, E. Hanelt, and B. A. Brown, Nucl. Phys. **A528**, 225 (1991).

[13] H. Ogawa, K. Asahi, K. Sakai, A. Yoshimi, M. Tsuda, Y. Uchiyama, T. Suzuki, K. Suzuki, N. Kurokawa, M. Adachi, H. Izumi, H. Ueno, T. Shimoda, S. Tanimoto, N. Takahashi, W.-D. Schmidt-Ott, M. Schäfer, S. Fukuda, A. Yoshida, M. Notani, T. Kubo, H. Okuno, H. Sato, N. Aoi, K. Yoneda, H. Iwasaki, N. Fukuda, N. Fukunishi, M. Ishihara, and H. Miyatake, Phys. Lett. **B451**, 11 (1999).

[14] G. Neyens, N. Coulier, S. Teughels, G. Georgiev, B. A. Brown, W. F. Rogers, D. L. Balabanski, R. Coussement, A. Lépine-Szily, M. Lewitowicz, W. Mittig, F. de Oliveira Santos, P. Roussel-Chomaz, S. Ternier, K. Vyvey, and D. Cortina-Gil, Phys. Rev. Lett. **82**, 497 (1999).

[15] G. D. Putt, L. K. Fifield, M. A. C. Hotchkis, T. R. Ophel, and D. C. Weisser, Nucl. Phys. **A399**, 190 (1983).

[16] F. C. Barker, Aust. J. Phys. **37**, 17 (1984).

[17] G. Duchêne, Nucl. Instrum. Methods A **432**, 90 (1999).

[18] Z. Elekes, T. Belgya, G. L. Molnár, Á. Z. Kiss, M. Csatlós, J. Gulyás, A. Krasznahorkay, and Z. Máté, Nucl. Instrum. Methods Phys. Res. A **503**, 580 (2003).

[19] A. Gavron, Phys. Rev. C **21**, 230 (1980).

[20] T. K. Alexander and J. S. Forster, *Advances in Nuclear Physics* (Plenum Press, New York, 1978), Vol. 10, Chap. 3.

[21] J. Billowes, E. G. Adelberger, O. Avila, N. A. Jelley, and W. R. Kolbl, Nucl. Phys. **A413**, 503 (1984).

[22] J. P. Allen, A. J. Howard, D. A. Bromley, and J. W. Olness, Nucl. Phys. **68**, 426 (1965).

[23] A similar analysis for $(d_{5/2})^3$ is given in I. Talmi, *Simple Models of Complex Nuclei, Contemporary Concepts in Physics* (Harwood Academic Publishers, Reading, UK, 1993) Vol. 7, p. 292.

[24] K. Sato, M. Tanigaki, T. Onishi, M. Fukuda, T. Minamisono, M. Mihara, K. Matsuta, S. Takeda, M. Sasaki, T. Yamaguchi, T. Miyake, K. Minamisoto, A. Morishita, F. Osumi, Y. Muramoto, S. Oui, T. Fukao, Y. Matsumoto, T. Ohtsubo, S. Fukuda, Y. Nojiri, S. Momota, K. Yoshida, A. Ozawa, T. Kobayashi, I. Tanihata, A. Kitagawa, M. Torikoshi, H. Sagawa, H. Kitagawa, G. F. Krebs, J. R. Alonso, and T. J. M. Symons, Nucl. Phys. **A654**, 735c (1999).

[25] A. Volya, Phys. Rev. C **65**, 044311 (2002).

[26] A. Volya and V. Zelevinsky, Phys. Rev. Lett. **94**, 052501 (2005).

[27] A. Volya and V. Zelevinsky, Phys. Rev. C **74**, 064314 (2006).

[28] E. K. Warburton and B. A. Brown, Phys. Rev. C **46**, 923 (1992).

[29] T. Otsuka, T. Suzuki, R. Fujimoto, H. Grawe, and Y. Akaishi, Phys. Rev. Lett. **95**, 232502 (2005).